BBA - Bioenergetics 1861 (2020) 148300

Contents lists available at ScienceDirect

BBA - Bioenergetics

journal homepage: www.elsevier.com/locate/bbabio

Metabolic rewiring in drug resistant cells exhibit higher OXPHOS and fatty acids as preferred major source to cellular energetics

Sameer Salunkhe[a,d,1], Saket V. Mishra[a,d,1], Atanu Ghorai[a], Aarti Hole[b], Pratik Chandrani[c], Amit Dutt[c,d], Murali Chilakapati[b,d], Shilpee Dutt[a,d,*]

[a] Shilpee Dutt Laboratory, Tata Memorial Centre, Advanced Centre for Treatment, Research and Education in Cancer (ACTREC), Kharghar, Navi Mumbai 410210, India
[b] Chilakapati Laboratory, Tata Memorial Centre, Advanced Centre for Treatment, Research and Education in Cancer (ACTREC), Kharghar, Navi Mumbai 410210, India
[c] Integrated Genomics Laboratory, Advanced Centre for Treatment Research Education in Cancer (ACTREC), India
[d] Homi Bhabha National Institute, Training School Complex, Anushakti Nagar, Mumbai 400085, India

ARTICLE INFO

Keywords:
Drug resistance
Lipid metabolism
OXPHOS
Mitochondria
Leukemia

ABSTRACT

Alteration in metabolic repertoire is associated with resistance phenotype. Although a common phenotype, not much efforts have been undertaken to design effective strategies to target the metabolic drift in cancerous cells with drug resistant properties. Here, we identified that drug resistant AML cell line HL-60/MX2 did not follow classical Warburg effect, instead these cells exhibited drastically low levels of aerobic glycolysis. Biochemical analysis confirmed reduced glucose consumption and lactic acid production by resistant population with no differences in glutamine consumption. Raman spectroscopy revealed increased lipid and cytochrome content in resistant cells which were also visualized as lipid droplets by Raman mapping, electron microscopy and lipid specific staining. Gene set enrichment analysis data from sensitive and resistant cell lines revealed significant enrichment of lipid metabolic pathways in HL-60/MX2 cells. Further, HL-60/MX2 possessed higher mitochondrial activity and increased OXPHOS suggesting the role of fatty acid metabolism as energy source which was confirmed by increased rate of fatty acid oxidation. Accordingly, OXPHOS inhibitor increased sensitivity of resistant cells to chemotherapeutic drug and fatty acid oxidation inhibitor Etomoxir reduced colony formation ability of resistant cells demonstrating the requirement of fatty acid metabolism and dependency on OXPHOS by resistant leukemic cells for survival and tumorigenicity.

1. Introduction

Acquired resistance is an evolutionary process during which cancer cells can revamp their survival dependencies to thrive adverse effects of chemotherapy. It is this change which makes drugs ineffective targeting a particular attribute. As evident from multiple studies the advanced stage resistance is multifactorial and to brought that in effect cancer cells need to modify their metabolic preferences. As explained by Warburg, cancer cells favor aerobic glycolysis over oxidative phosphorylation to drive their energy requirements [1] however, we now know that under stress cancer cells are likely to alter their metabolic preferences to gain survival advantage. Therefore, it is indeed important to target these metabolic alterations to counteract the survival gain by drug resistant cells by metabolic rewiring.

Apart from glucose, different cancer cells under different physiological contexts have been shown to prefer plethora of substrates as their energy source such as glutamine, lactate [2], pyruvate and fatty acids. Previously it has been shown that drug resistant cells with mitochondrial defects tend favor increased glycolysis, and inhibition of it leads to sensitization of such cells [3,4]. While Thomas et al. used AML patient samples and mouse model to demonstrate that drug resistant population show increased OXYPHOS and inhibition of fatty acid metabolism causes reversal of drug resistance [5]. Although previous studies have reported alteration in metabolic preferences by leukemic cells, it's still not very well understood and is of course far from its application in the treatment of drug resistant leukemias. We observed a contrasting phenotype between AML HL-60 and its mitoxantrone resistant subline HL-60/MX2. HL-60 alike most of the AML cells changed culture medium

Abbreviations: OXPHOS, Oxidative phosphorylation; OCR, Oxygen consumption rate; GSEA, Gene set enrichment analysis; ROS, Reactive oxygen species; AMA, Antimycin-A

* Corresponding author at: KS 326, Tata Memorial Centre, ACTREC, Navi Mumbai, Maharashtra, India.
E-mail address: sdutt@actrec.gov.in (S. Dutt).

[1] These authors contribute equally to this work

https://doi.org/10.1016/j.bbabio.2020.148300
Received 22 August 2019; Received in revised form 10 August 2020; Accepted 21 August 2020
Available online 25 August 2020

color to yellow after 48 h culture while HL-60/MX2 remained reddish pink. In our study we pursued this key observation by taking multiple relevant approaches like transcriptome analysis and Raman spectroscopy, clubbed with biochemical and microscopic analysis to figure out increased fatty acid content and its oxidation as a source of energy to drug resistant cells. Inhibition of OXPHOS and fatty acid oxidation pathway lead to significant reduction in proliferation of HL-60/MX2 cells and further treatment with mitoxantrone stimulated cell death in these extremely drug resistant cells.

2. Materials and methods

2.1. Cell lines and growth conditions

HL-60 and THP-1was procured from National Centre for Cell Science (NCCS), Pune and HL-60/MX2 was purchased from ATCC. THP1-D7 resistant cell line was developed in the lab according to protocol mentioned in Salunkhe et al. [14]. All cell lines were grown in complete RPMI containing 10% FBS and 1% antibiotic cocktail (Penstrep).

2.2. Proliferation and viability assay

Trypan blue viability staining was done to count number of viable and dead cells to calculate proliferation as well as cell death post drug treatment. Drugs- Mitoxantrone (Sun pharmaceuticals), Etomoxir (Ab144763), Antimycin-A (Sigma A8674).

2.3. Estimation of glucose and lactate

0.5 *10^6 cells were seeded in complete RPMI media with 10% FBS. To measure the glucose and lactate in extracellular medium, 500uL of cell suspension was spun down and clear soup was collected after seeding and 24, 48, and 72 h post seeding. Glucose and lactate in supernatant were measured using (Dimensions RXL Siemens) ACTREC pathology.

2.4. Raman mapping

Raman spectra of single HL60 and MX2 cells fixed in PFA, were acquired using WITec Raman alpha300R (WITec, GmbH) confocal Raman microscope. Raman microscope Wavelength of 532 nm at 8 mW power was used for excitation through a 100 X objective (Zeiss, 1.46 N.A.) on a single cell. Raman scattered photons were collected through a 50 μm fiber and directed to a 300 mm spectrograph equipped with 1200 g/mm grating and thermo-cooled CCD. Spectra were acquired over 500 to 2200 cm^{-1} range. For conducting experiments, a grid consisting of 20 × 20 pixels and covering an area of 18 × 18 μm was selected over the visible light image and 400 spectra/ map with integration time of 25 s/spectrum and resolution of 0.75 μm were acquired. Preproccessed (base-line correction, vector normalization and interpolated) spectra were subjected K-means cluster analysis (KCA) using WITec project four software was employed to generate pseudo color Raman maps.

2.5. Raman point spectroscopy

Spectra of cell pellets of HL60 and MX2 cell lines washed thrice in buffered saline and fixed in 70% ethanol were recorded using a commercial Raman microscope, (WITec alpha300R, λx-532 nm, 8 mW, 600 grooves/mm, 10 s acquisition and 10 integrations, cm^{-1}). Typically, 20 spectra, at different positions on the cell pellets, were collected per each pellet. Spectra were collected triplicate of three different experiments were used for analysis. Preprocessed spectra, baseline corrected, interpolated and vector normalized were analyzed (PCLDA) by Commercial Unscrambler® X software was employed for data analysis.

2.6. Electron microscopy

Briefly, exponentially growing 10 million cells (HL-60 and HL-60/MX2) were pelleted down and washed twice with phosphate buffered saline. 1 ml of 3% glutaraldehyde (Fixative) was slowly added to the pellet and kept at 4^0C for 2 h. Cells were again centrifuged to remove the fixative and washed twice with 1 ml of 0.1 M Sodium cacodylate buffer and stored in 4^0C prior to submission in ACTREC electron microscopy facility.

2.7. Oil Red O staining

Exponentially growing cells were fixed in 10% formalin for 30 min. Cells were then washed twice with PBS. Cell pellet was added with 60% isopropanol and incubated for 5 min. Cells were then spread on a clean grease free slide in a monolayer and allowed to air dry. 2 ml of prewarmed Oil red O stain (at 60 °C) was evenly overlaid on the cell smear and kept for 5 min. Slides were then washed with water to clear excess of stain. Slides were mounted with a coverslip and observed under inverted microscope.

2.8. Mitotracker assay

0.5*10^6 exponentially growing cells were seeded in a glass bottom petri dish and treated with 50 nM of mitotracker dye (MitoTracker® Green FM) and incubated for 30 min in dark for 30 min in CO2 incubator. Medium was replaced with fresh growth medium and cells were imaged on confocal microscope using green channel settings (Ex-490, Em-516).

2.9. Extracellular oxygen consumption assay

For detailed protocol follow abcam protocol manual for ab197243. Briefly 50000 cells were seeded in 100uL of 10% FBS containing RPMI medium. Duplicate reactions were set up for reaction controls like glucose oxidase and antimycin. Oxygen consumption reagent was added to each well and overlaid with high sensitivity mineral oil. Microplate fluorescence reader (Biotek cytation 5) was used to record the fluorescence for 4 h.

2.10. Extracellular Flux Analyzer

To analyze the mitochondrial OXPHOS under normal physiological condition between HL-60 and HL-60/MX2, we used Seahorse XF24 Extracellular Flux Analyzer (Seahorse Biosciences, USA) according to the protocol mentioned by the manufacturer. In brief, 2*10^5 cells were seeded in each well on previous day and incubated in CO2 incubator at 37 °C for overnight. Next day prior to loading onto the Seahorse XF24 analyzer, the plate was kept in non-CO_2 incubator at 37 °C for 40 min in freshly prepared base medium (DMEM, pH- 7.4; supplemented with 10 mM glucose, 4 mM L-glutamine and 1 mM sodium pyruvate) as provided by the Seahorse Biosciences, USA. To get the real time changes, oligomycin (1 μM), FCCP (1 μM), and rotenone (1 μM) were injected sequentially. Finally, the mitochondrial OXPHOS was measured as oxygen consumption rate (OCR in pmol/min) for each cell type and it was normalized by protein content as detected by Pierce BCA Protein Assay reagent (Thermo Fisher Scientific Inc., USA). From the three biological independent bioenergetics profiles of HL-60 vs HL-60/MX2, several parameters like basal respiration, maximal respiration, spare respiratory capacity, ATP production, proton leak and non-mitochondrial oxygen consumption were determined. Data are shown as mean ± standard error of mean (SEM) of three independent experiments. Student's *t*-test is used to calculate the significant differences between two groups of data and represented as '*' ($0.05 > P > 0.01$) and '**' ($0.01 \geq P > 0.001$).

2.11. ROS analysis

To analyze the cellular reactive oxygen species (ROS) level 2′-7′-Dichlorodihydrofluorescein diacetate (DCFH-DA) was used. DCFH-DA is cell permeable compound which gets oxidized by ROS into green fluorescent compound 2′-7′-Dichlorofluorescein (DCF). 25,000 cells per 100 μl were seeded of 10% FBS containing RPMI medium in 96 well plate. Cells were incubated with 1 mM hydrogen peroxide for 30 min followed by 30 min incubation in dark with 5 μM DCFH-DA in 37 °C CO_2 incubator. Microplate fluorescence reader (Biotek cytation 5) was used to record the fluorescence at excitation 495 nm and emission 529 nm wavelength.

2.12. Gene set enrichment analysis

Whole transcriptome sequencing data analysis were performed as described earlier [6,7]. The differentially expressed genes were analyzed through fold-change based pre-ranked GSEA tool [8] for lipid metabolism pathways available from GSEA website. The *p*-value and FDR q-value cut-off of 0.05 was used for assessment.

2.13. Fatty acid oxidation assay

Find detailed protocol (ab217602 Fatty Acid Oxidation Assay). In brief 50000 cells were seeded in 100 μl glucose deprivation medium in a 96 well plate. Next day replace the medium with FA-free (only glucose) and FA measurement media (glucose with 18C unsaturated fatty acid Oleate as substrate). Necessary controls like (Etomoxir, FCCP and glucose oxidase and oxygen consumption reagent) were included in duplicate reactions. Reaction was overlaid with high sensitivity mineral oil. Microplate fluorescence reader (Biotek cytation 5) was used to record the fluorescence for 3 h.

2.14. Clonogenic assay

1×10^3 cells were treated with drug and seeded directly in 500 μl of 1.6% methyl cellulose agar (MCM) with equal amount of 2× RPMI containing 20% FBS (cells treated with Etomoxir were seeded in MCM and 2× RPMI with 50 μM of Etomoxir). Colonies (> 20 cells) were scored under inverted optical microscope (Olympus model IX 51) on the 15th day. Data are shown as mean ± standard error of mean (SEM) of three independent experiments. Student's *t*-test is used to calculate the significant differences between two groups of data.

3. Results

3.1. Mitoxantrone resistant HL-60/MX2 does not follow classical Warburg effect

We explored HL-60 and HL-60/MX2 (mitoxantrone resistant HL-60) to elucidate the metabolic differences associated with chemoresistance. We first confirmed resistance of HL-60/MX2 cells to mitoxantrone drug (Fig. 1A). We observed that, when seeded in RPMI media at equal cell density, the doubling times of HL-60 and HL-60/MX2 remains similar based on cell count taken on 24 h, 48 h and 72 h. (Fig. 1B). Strikingly, HL-60 showed a change in the color of extracellular media from reddish pink to yellow by 48–72 h, in contrast HL-60/MX2 cells do not show alteration in media color (Fig. 1C). The difference in the change in the media coloration was consistently observed even after multiple passages. Although we do not clearly understand this but cancerous cells prefer less energy efficient aerobic glycolysis over OXPHOS in the presence of abundant oxygen, however accumulation of lactic acid succeeding an exponential growth is commonly observed in a cell culture system [9]. Phenol red a pH indicator used in growth medium changes its color from reddish pink to yellow as acids are secreted out in extracellular medium. Following the observation where only HL-60 cells showed such phenotype we assumed possibility of differential extracellular secretion of lactic acid in HL-60 and HL-60/MX2 cells. We therefore estimated the levels of extracellular lactic acid in fresh, and spent media (on 24 h,48 h and 72 h) following seeding at equal cell density. As predicted in HL-60 lactate levels post 72 h culture were almost 6-fold higher than that of HL-60/MX2 cells (Fig. 1D). Cancer cell typically follow classical Warburg effect where in large quantities of glucose are metabolized via aerobic glycolysis to harness the energy for cellular growth and proliferation [1]. Hence, we estimated the rate of glucose consumption by HL-60 and HL-60/MX2 cells at similar time points like lactate production. The rate of glucose consumption was consistently higher in HL-60 cells than HL-60/MX2 cells as observed till 72 h (Fig. 1e). In fact, HL-60/MX2 cells showed minor glucose consumption compared to HL-60 indicating reduced dependency on glucose in drug resistant cells. To further confirm the same, we analyzed the transcript levels of *GLUT1*, *HIF1A* and *PKC* zeta i.e. genes that are positively associated with glycolytic phenotype. We observed a significant downregulation in the transcript levels of all these genes (Fig. 1f) which also suggest reveres Warburg effect likely to be followed by HL-60/MX2 cells. Additionally, we also analyzed another leukemic cell line THP1 and its resistant counterpart (THP1- D7) generated in our lab as previously describes [14] for pH of spent media, lactate production and glycolysis factors expression levels. As shown in supplementary Fig. 1a–c results were consistent with that from HL60 and HL-60/MX2 cell line where resistant cells showed high pH, decreased lactate production and decreased mRNA expression of glycolysis factors (*Pkcz, Glut1, HIF-1A*).

3.2. Drug resistant cells show increased lipids content

Glutamine metabolism is known to aid cancer cells maintain their proliferation under stress conditions [10]. As glucose wasn't significantly utilized by HL-60/MX2 cells, we monitored the proliferation and mitoxantrone sensitivity of HL-60 and HL-60/MX2 cells in RPMI complete media with and without glutamine. We found insignificant differences in either proliferation (Fig. 2A) or sensitivity (Fig. 2B) to mitoxantrone in HL-60/MX2 cells cultured in glutamine free media ruling out the possibility of glutamine as key source of energy for HL-60/MX2. Next, we focused to understand the gross differences in the metabolic repertoire of HL-60 and HL-60/MX2 cells. Raman spectroscopy has been widely used to monitor the biochemical composition in intact cells this not only helps in quantitating metabolite differences, but also helps in determining their local concentrations using mapping methods [11]. Typical pseudo color Raman maps generated using KCA, employing 5 clusters, of HL60 and MX2 along with respective white pictograph are shown in Fig. 2C. Average spectra of different clusters of the Raman maps, also shown in the Fig. 2C, indicate presence of biomolecules such as DNA (780 cm^{-1}, 1130 cm^{-1}), Proteins (1250 cm^{-1}, 1450 cm^{-1} and 1650 cm^{-1}) and lipids (1740 cm^{-1}). As can be seen from these spectral features, spectra of the most clusters of MX2 show abundance of lipids unlike their wild type HL-60 counter parts.

Following the evidences from Raman data we decided to perform transmission electron microscopy to detect the differences in subcellular architecture of both the cell types. Cells in their normal physiology did not show drastic differences in mitochondrial size, shape or numbers however there were striking differences in the lipid droplet like structures in resistant cells. In drug resistant cells lipid droplets were not only greater in number but also slightly larger in size when compared to drug sensitive cells (Fig. 2D). Increased numbers of lipid droplets were further confirmed by oil red O staining (Supplementary Fig. 2a).

3.3. HL-60/MX2 cells exhibit efficient bioenergetics through competent OXPHOS

Acknowledging the differences in biochemical and Raman

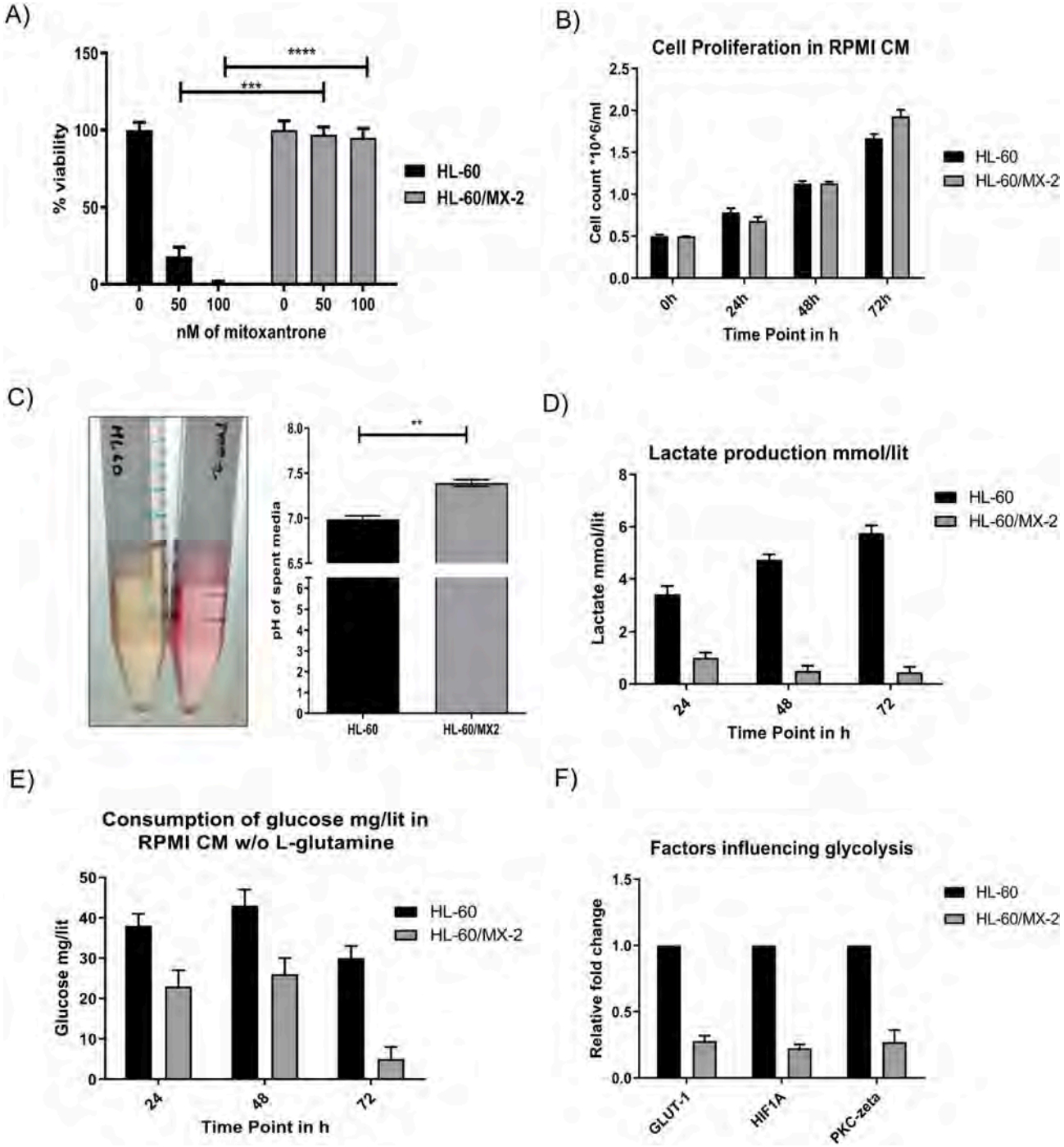

Fig. 1. A) Trypan blue viability counting of HL-60 and HL-60/MX2 cells post mitoxantrone treatment. Cellular proliferation of HL-60 and HL-60/MX2 cells in RPMI complete medium. B) Change in the pH of extracellular medium post 48 h of culture. C) Lactate production mmol/lit post 24 h, 48 h and 72 h in both the cell lines. D) Glucose consumption (mg/lit) in both the cells at 24 h, 48 h and 72 h of culture. E) qPCR for GLUT-1, HIF1A and PKC-zeta expression in exponentially growing culture. Student's *t*-test is used to calculate the significant differences between two groups of data and represented as '*' ($0.05 > P > 0.01$) and '**' ($0.01 \geq P > 0.001$).

spectrometry data we considered looking into mitochondrial activity of these cells. We used mitotracker dye to visualize and quantitate the differences in mitochondrial activity. We observed a higher mitochondrial activity in HL-60/MX2 cells (Fig. 3A) however, higher rate of mitochondrial activity could only confirm higher mitochondrial respiration rate. Also, higher mitochondrial activity supports Raman spectrometry data of increased cytochrome content which suggests elevated mitochondrial efficiency however, we were still clueless about source of energy for drug resistant cells. Assuming lipid droplets could serve as fuel reserves for MX2 cells which are metabolized within mitochondria. We first measured the cellular respiration by measuring the depletion of extracellular oxygen as oxygen consumption rate (OCR) of both cell types in order to understand the bioenergetics. OCR was measured in normal growth conditions using fluorescent dye which quenches in the presence of extracellular oxygen. We observed exponential increase in OCR in both the cell types until certain point, following which only HL-60/MX2 cells displayed a saturation in OCR rate in contrary to HL-60 cells which kept on following continuous

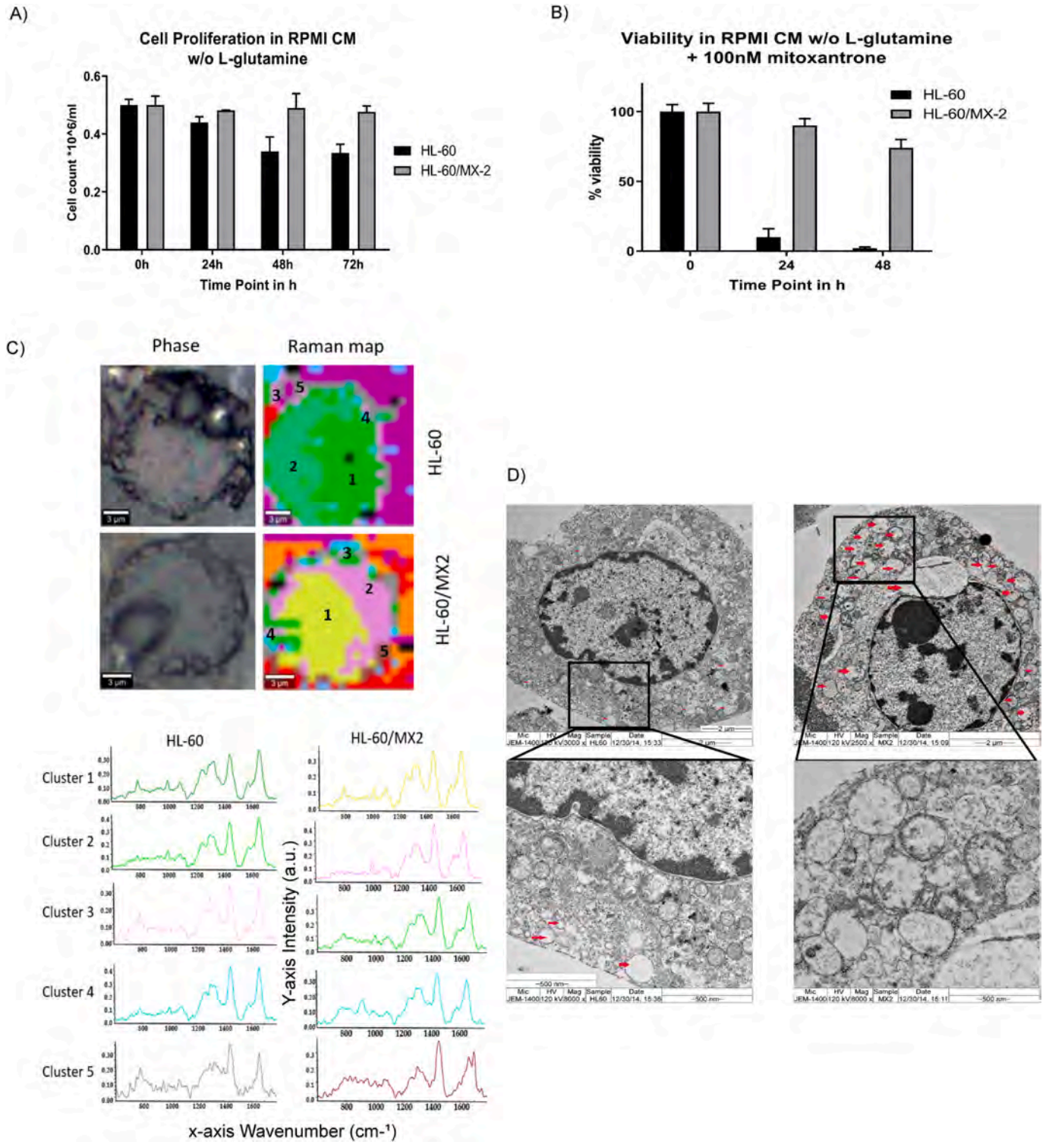

Fig. 2. A) Cellular proliferation of HL-60 and HL-60/MX2 cells in RPMI complete medium without L-glutamine. B) Trypan blue viability counting of HL-60 and HL-60/MX2 cells cultured in L-glutamine free RPMI medium post mitoxantrone (100 nM Conc.) treatment. C) Phase contrast images of HL 60 cell and HL-60/MX2 cells and 5-cluster pseudo color Raman map for both the cell lines. Graphs on right represents average spectrum of Cluster I, Cluster II, Cluster III, Cluster IV and Cluster V. D) Transmission electron micrograph for HL-60 and HL-60/MX2 cells (Upper layer images have scale of 2 μm and magnification of 2500×, lower layer has 8000× magnified image of above having scale of 500 nm).

oxygen consumption (Fig. 3B). Similarly, THP-1 D7 cells also showed low OCR compared to their sensitive counterpart (THP-1) (Supplementary Fig. 1d). This data in coordination with mitochondrial activity and cellular proliferation suggests that drug resistant cells are able to achieve similar growth rates with higher mitochondrial efficiencies and optimum oxygen consumption. Undue OCR rates (Hyperoxia) can lead to generation ROS which needs to be controlled to reduce toxic side effects [12]. We also observe increased level of ROS in resistant cells (Supplementary Fig. 4a). To analyze the mitochondrial activity differences thoroughly, we performed mitochondrial respiration assay using

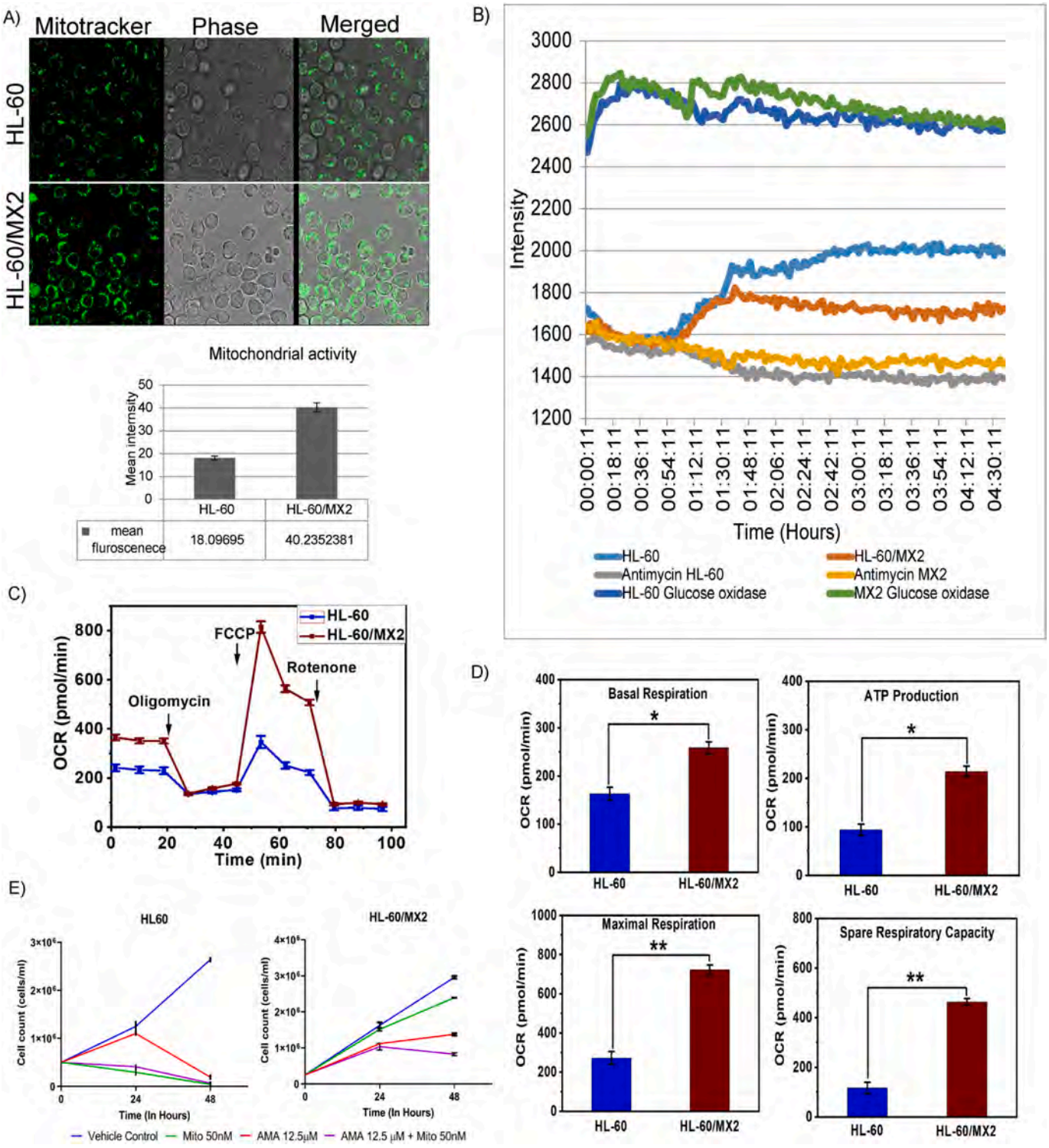

Fig. 3. A) Confocal images for mitotracker dye staining in HL-60 and HL-60/MX2 cells. Graph represents average intensity per 20 cells. B) Total Cellular oxygen consumption measured as oxygen consumption rate in RPMI complete medium. C) Measurement of total mitochondrial respiration as oxygen consumption rate using seahorse method. D) Graphs representing mitochondrial – basal respiration, ATP production, maximal respiration and spare respiration capacity. E) Trypan blue count of HL-60 and HL-60/MX2 cells after 24 h and 48 h treatment of 12.5uM antimycin-a (AMA) and mitoxantrone (Mito) (50 nM) alone and in combination. Student's *t*-test is used to calculate the significant differences between two groups of data and represented as '*' ($0.05 > P > 0.01$) and '**' ($0.01 \geq P > 0.001$).

seahorse method to measure important parameters like basal respiration, maximum respiration, ATP production, spare capacity and proton leak (Fig. 3C and D). Interestingly, HL-60/MX2 shows significantly higher basal respiration than its sensitive counterpart HL-60 under normal physiological condition. Consequently, it produces higher ATP during OXPHOS. As expected, HL-60/MX2 cells showed significantly higher maximal respiration and spare respiratory capacity than HL-60 when oxidative phosphorylation is uncoupled by using chemical uncoupler FCCP and followed by total shut down of ETC (electron transport chain) by rotenone. We have also determined proton leak and non-mitochondrial oxygen consumption but we couldn't observe any significant differences between these two cell types (Supplementary

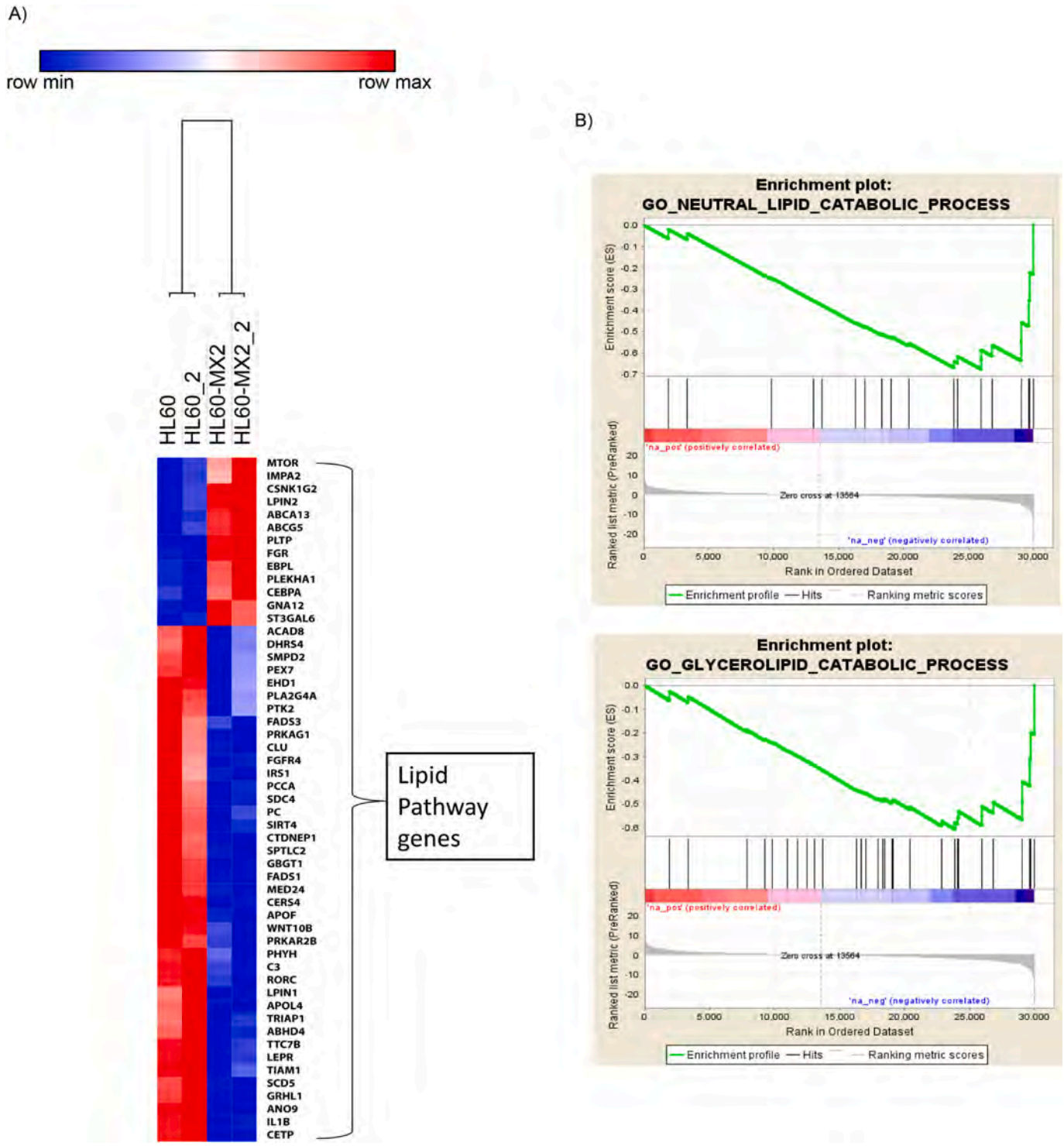

Fig. 4. A) Heatmap of lipid pathway gene expression data obtained from RNAseq analysis of HL-60 and HL-60/MX2 cells. B) The differentially expressed genes were analyzed through fold-change based pre-ranked GSEA tool for lipid metabolism pathways available from GSEA website. RNAseq data was from biological triplicate experiment. The *p*-value and FDR q-value cut-off of 0.05 was used for assessment.

Fig. 4b and c). To further confirm the causative relationship between oxidative metabolism and drug resistance, we inhibited OXPHOS by Antimycin-A (AMA), an inhibitor of ETC-Complex III. HL-60/MX2 cells shows significant increase to mitoxantrone susceptibility in combination with AMA compared to the mitoxantrone alone highlighting the importance of OXPHOS to the resistance. The effect of AMA alone, however, was stronger on HL-60 cells as compared to HL-60/MX2 cells. These results were expected as it is reported that HL-60/MX2 cells have constitutively high expression of anti-apoptotic proteins such as MCL1 [13] along with other multifactorial drug resistance mechanism which resist apoptosis induction [14]. Again, the HL-60/MX2 cells have higher mitochondrial activity, therefore it was expected that they need higher doses of AMA as well to exhibit significant cell death. On the other hand HL-60 cells unlike most of the cancer cells utilizes OXPHOS to support normal growth by switching between glucose and glutamine [15] to harness energy which does not strictly follow the Warburg effect

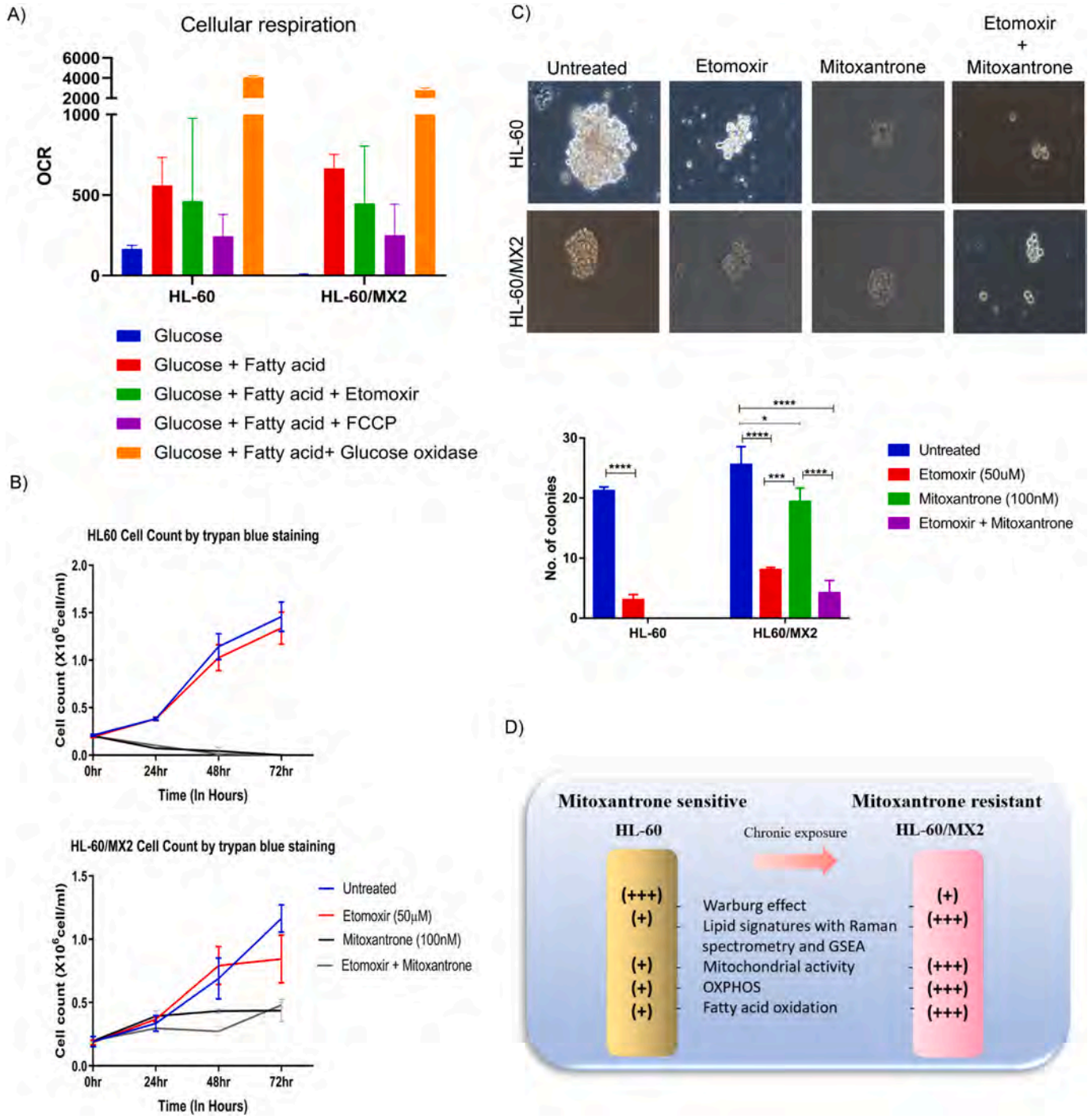

Fig. 5. A) Measurement of total cellular respiration as oxygen consumption rates with different combination of glucose, glucose + oleic acid with Etomoxir, FCCP and Glucose oxidase. B) Effect of Inhibitor of fatty acid transporter (CPT1) on cellular proliferation with and without mitoxantrone measured by trypan blue staining. C) Representative images of a HL-60 and HL-60/MX2 cell colony observed by bright-field microscopy (20× objective) at day 15 of growth in soft agar (Scale bar = 50 um). Bar graph quantifies the number of colonies formed in different cell populations after Etomoxir treatment. Results in each bar and line graph are the composite data from three independent experiments performed in triplicate (mean ± SEM); * denotes p.05, ** denotes p.01 and *** denotes p.001. D) Model for metabolic rewiring in HL-60/MX2 cells.

making them susceptible to AMA treatment.

3.4. Gene expression data-GSEA analysis reveals enrichment of lipid metabolic pathways

In a parallel analysis of gene expression data from both HL-60 and HL-60/MX2 cells we dug into comparison of gene set enrichment for various metabolic pathways in both the cell types. RNA seq data was used to perform gene set enrichment analysis for 67 known lipid metabolic pathways in both the cell types. The results show overall up-regulation and downregulation of subset of lipid pathway genes (Fig. 4 and Supplementary Fig. 5), however, only two pathways (Gene Ontology based neutral lipid catabolic pathway and glycerolipid catabolic pathway) were statistically significantly downregulated in resistant cells (Fig. 4B and Supplementary Figs. 6 and 7). Downregulation of various lipid catabolic genes are in-line with increases lipid content in

the resistant cells, further support by independent observation of higher lipid content in aggressive cancer cells [16].

Drug resistant cells preferentially utilize fatty acids over glucose, contributing to drug resistance property.

Gene expression, Raman and electron microscopy data hints towards use of lipids as an energy source by resistant cells. To confirm this observation, we performed fatty acid oxidation assay on both the cell types. Cells were added with controlled quantities of glucose and in combination with oleic acid as fatty acid source and measured oxygen consumption rates (OCR) to interpret their utilization kinetics. We included additional controls like Etomoxir, FCCP and glucose oxidase to evaluate the assay efficiency. We confirmed minimum OCR in drug resistant HL-60/MX2 cells with only glucose in base media. However, in presence of oleic acid the OCR were almost similar to that of HL-60 (Fig. 5A). This endorses the preference of fatty acids over glucose in HL-60/MX2 cells. Addition of Etomoxir (Inhibitor of fatty acid transport in mitochondria) or FCCP (Inhibitor of mitochondrial ATP synthesis) slashed OCR drastically in both type of cells. Next, to understand if inhibition of mitochondrial fatty acid transporter (CPT1) can weaken metabolic regulation of drug resistant cells and sensitize them to DNA damaging drug; We treated both the cell types with Etomoxir prior to mitoxantrone treatment and measured % viability at different points post drug treatment. 50 μM of CPT1 inhibitor-Etomoxir treatment up to 72 h did not have any effect on resistant cell viability (Fig. 5B). However, upon long term treatment with same concentration of drug resulted in significant decrease in colony forming capacity (Fig. 5C).

4. Conclusions

Drug resistance is ever growing problem with varieties of cancer targeting drugs. In order to survive through drug pressure, cancerous cells evolve one or more survival mechanisms [17].In such cases changes in fundamental physiological pathways demand twists in metabolic aspects of a cell. Blocking such alterations weakens cells ability to adapt new changes and can benefit in bringing better outcomes with chemotherapy. Previous studies have well described such change in metabolic phenotype however, its needs more substantial evidences and translational aspects to move into cancer therapeutics. In our study we implemented relevant methodologies to define the metabolic changes in drug resistant cells, which would be important in developing newer strategies to deal with highly drug resistant tumors. We identify importance of OXPHOS and fatty acid metabolism in offering survival advantage to the drug resistant cell (Figs. 3E and 5C). These cells show increased lipid deposits in the form of lipid droplets coupled with enrichment of lipid metabolism pathways and show great metabolic activities achieved under low overall oxygen consumption which might help in overcoming ROS related toxicities. Increase in vulnerability to anthracyclines in resistant cells upon acute inhibition of OXPHOS by Antimycin-A and chronic exposure of fatty acid oxidation inhibitor like Etomoxir exhibit the presence of preferential oxidative phosphorylation when compared to aerobic glycolysis and increased rate of fatty acid oxidation. Findings from this work leads to more stimulating questions such as what is the intricate mechanism of the metabolic shift and also how the metabolic preferences are regulated for different energy molecules.

Financial support

This work was supported by Indian Council of Medical Research (grant no. 90/04/2012-STM(TF)/BMS) to Dr. Shilpee Dutt. S·S is CSIR fellow. AG is DST-SERB, NPDF (PDF/2016/00158) and S.V.M is a DBT fellow. The authors declare no competing financial interests.

CRediT authorship contribution statement

SS and SD conceptualized the study. SS, AG, SVM, AH performed experiments. PC performed the bioinformatics analysis with inputs from AD. SD and SS analyzed the data. SD and SS wrote the manuscript with inputs from MC. SD supervised the study.

Declaration of competing interest

Authors declare no conflict of interests.

Acknowledgements

We thank Dr. Preeti Chavan, Officer-In-Charge, ACTREC Composite pathology lab for helping us with metabolite analysis. We also acknowledge Dr. Ullas Kothur, TIFR Mumbai for providing Seahorse XF24 Extracellular Flux Analyzer facility.

RNAseq data availability

RNA-seq data is deposited in the ArrayExpress database at EMBL-EBI (http://www.ebi.ac.uk/arrayexpress/experiments/E-MTAB-8981) under accession number E-MTAB-898.

Appendix A. Supplementary data

Supplementary data to this article can be found online at https://doi.org/10.1016/j.bbabio.2020.148300.

References

[1] O. Warburg, On the origin of cancer cells, Science. 123 (3191) (1956) 309–314.
[2] S. Park, C.Y. Chang, R. Safi, X. Liu, R. Baldi, J.S. Jasper, et al., ERRalpha-regulated lactate metabolism contributes to resistance to targeted therapies in breast cancer, Cell Rep. 15 (2) (2016) 323–335.
[3] Z. Derdak, N.M. Mark, G. Beldi, S.C. Robson, J.R. Wands, G. Baffy, The mitochondrial uncoupling protein-2 promotes chemoresistance in cancer cells, Cancer Res. 68 (8) (2008) 2813–2819.
[4] R.H. Xu, H. Pelicano, Y. Zhou, J.S. Carew, L. Feng, K.N. Bhalla, et al., Inhibition of glycolysis in cancer cells: a novel strategy to overcome drug resistance associated with mitochondrial respiratory defect and hypoxia, Cancer Res. 65 (2) (2005) 613–621.
[5] T. Farge, E. Saland, F. de Toni, N. Aroua, M. Hosseini, R. Perry, et al., Chemotherapy-resistant human acute myeloid leukemia cells are not enriched for leukemic stem cells but require oxidative metabolism, Cancer Discov. 7 (7) (2017) 716–735.
[6] P. Chandrani, P. Upadhyay, P. Iyer, M. Tanna, M. Shetty, G.V. Raghuram, et al., Integrated genomics approach to identify biologically relevant alterations in fewer samples, BMC Genomics 16 (2015) 936.
[7] S. Salunkhe, N. Chandran, P. Chandrani, A. Dutt, S. Dutt, CytoPred: 7-gene pair metric for AML cytogenetic risk prediction, Brief. Bioinform. 21 (1) (2018) 348–354, https://doi.org/10.1093/bib/bby100.
[8] A. Subramanian, P. Tamayo, V.K. Mootha, S. Mukherjee, B.L. Ebert, M.A. Gillette, et al., Gene set enrichment analysis: a knowledge-based approach for interpreting genome-wide expression profiles, Proc. Natl. Acad. Sci. U. S. A. 102 (43) (2005) 15545–15550.
[9] M.G. Vander Heiden, L.C. Cantley, C.B. Thompson, Understanding the Warburg effect: the metabolic requirements of cell proliferation, Science. 324 (5930) (2009) 1029–1033.
[10] Y.K. Choi, K.G. Park, Targeting glutamine metabolism for cancer treatment, Biomol Ther (Seoul). 26 (1) (2018) 19–28.
[11] J.L. Griffin, J.P. Shockcor, Metabolic profiles of cancer cells, Nat. Rev. Cancer 4 (7) (2004) 551–561.
[12] J.L. Campian, M. Qian, X. Gao, J.W. Eaton, Oxygen tolerance and coupling of mitochondrial electron transport, J. Biol. Chem. 279 (45) (2004) 46580–46587.
[13] D.L. Hermanson, S.G. Das, Y. Li, C. Xing, Overexpression of Mcl-1 confers multidrug resistance, whereas topoisomerase IIbeta downregulation introduces mitoxantrone-specific drug resistance in acute myeloid leukemia, Mol. Pharmacol. 84 (2) (2013) 236–243.
[14] W.G. Harker, D.L. Slade, W.S. Dalton, P.S. Meltzer, J.M. Trent, Multidrug resistance in mitoxantrone-selected HL-60 leukemia cells in the absence of P-glycoprotein overexpression, Cancer Res. 49 (16) (1989) 4542–4549.
[15] J.M. Garcia-Heredia, A. Carnero, Decoding Warburg's hypothesis: tumor-related mutations in the mitochondrial respiratory chain, Oncotarget. 6 (39) (2015) 41582–41599.
[16] T. Tomin, K. Fritz, J. Gindlhuber, L. Waldherr, B. Pucher, G.G. Thallinger, et al., Deletion of adipose triglyceride lipase links triacylglycerol accumulation to a more-aggressive phenotype in A549 lung carcinoma cells, J. Proteome Res. 17 (4) (2018) 1415–1425.
[17] S. Salunkhe, S.V. Mishra, J. Nair, S. Ghosh, N. Choudhary, E. Kaur, et al., Inhibition of novel GCN5-ATM axis restricts the onset of acquired drug resistance in leukemia, Int. J. Cancer 142 (10) (2018) 2175–2185.